

# Stability of multiply charged fullerene ions

P. Scheier<sup>1</sup>, B. Dünser<sup>1</sup>, G. Senn<sup>1</sup>, H. Drexel<sup>1</sup>, HP. Winter<sup>2</sup>, F. Aumayr<sup>2</sup>, G. Betz<sup>2</sup>, F. Biasioli<sup>1</sup>, T. Fiegele<sup>1</sup>, and T.D. Märk<sup>1</sup>

<sup>1</sup>Institut für Ionenphysik, Universität Innsbruck, Technikerstrasse 25, A-6020 Innsbruck, Austria

<sup>2</sup>Institut für Allgemeine Physik, Technische Universität Wien, A-1040 Wien, Austria

Received: 18 September 1998 / Received in final form: 19 February 1999

**Abstract.** Spontaneous (metastable) and surface-induced decay reactions for multiply charged fullerene ions, investigated recently in Innsbruck, are reviewed. Results discussed include the mechanisms and energetics of C<sub>2</sub> evaporation and charge separation reactions, the secondary electron emission upon impact on gold surfaces, and surface-induced reactions of singly and multiply charged fullerene ions.

**PACS.** 36.40.Qv Stability and fragmentation of clusters – 81.05.Tp Fullerenes and related materials; diamonds, graphite

## 1 Introduction

From the very first experiments performed right after the discovery of the Buckminster fullerene in 1985 [1], the stability of these molecules has turned out to be exceptionally high. In contrast to molecules of comparable size, fullerenes in general, and in particular, the fascinating C<sub>60</sub> molecule, can be exposed to external forces and stress without causing destruction of the cage. For instance, in the case of collisions with clean metallic surfaces, fullerenes bounce back almost elastically up to impact energies of 300 eV (which corresponds to a velocity of about 10 km/s) [2]. Furthermore, in an oven, C<sub>60</sub> can be heated up to about 1200 K without being destroyed [3]. Moreover, for electron impact ionization, only at electron energies larger than about 45 eV can dissociative ionization reactions be observed for time scales of several μs [4]. Finally, C<sub>60</sub> can be charged up to  $z = 9+$  without being destroyed in a Coulomb explosion [5, 6].

Until recently, the “fullerene community” was split into two groups concerning the question of the dominant fragmentation mechanism for fullerene ions C<sub>60</sub><sup>z+</sup> decaying into fragments with sizes below C<sub>58</sub><sup>z+</sup>; i.e., whether it is a fission-like process splitting the fullerene into two fragments or a sequential C<sub>2</sub> evaporation mechanism leading to the final dissociation products. From an energetic point of view, the first process should be more likely, but statistical arguments are in favor of the second type of decay [7]. Recent results from our laboratory elucidating this question and related topics will be summarized in this review. It is interesting to note in this context that Opitz and Huber [8] recently measured correlations between fragment

ions for C<sub>60</sub><sup>z+</sup> generated through collisions of C<sub>60</sub> with multiply charged ion beams.

## 2 Metastable decay reactions

Figure 1 shows a mass-analyzed ion kinetic energy (MIKE) spectrum of the C<sub>60</sub><sup>4+</sup> parent ion that was created by electron impact ionization. It should be mentioned that the primary ion signal had to be corrected due to a coincidence with the fragment ion C<sub>15</sub><sup>+</sup>, which has the same mass-per-charge ratio. This was done by the analysis of the isotopic peak pattern of the mass peaks [9]. On the left side of the parent ion signal there are two peaks, which indicate the formation of the fragment ions C<sub>58</sub><sup>4+</sup> and C<sub>56</sub><sup>4+</sup>, respectively. It is not possible to determine in the present case whether the C<sub>56</sub><sup>4+</sup> ion is created by the emission of a single C<sub>4</sub> unit or by the successive ejection of two C<sub>2</sub> fragments. On the right side of the parent ion there are three peaks visible, which are the result of the decay of C<sub>60</sub><sup>4+</sup> into C<sub>58</sub><sup>3+</sup>, C<sub>56</sub><sup>3+</sup>, and C<sub>54</sub><sup>3+</sup>, respectively. In these charge separation reactions, two ions are formed; therefore, it might be possible to measure also the second, much lighter fragment ion in a MIKE scan.

The large peak width of the fragment ions with lower charge state than the precursor ion in Fig. 1 indicates the presence of a large kinetic energy release (KER) in these decays. The Coulomb repulsion between the two fragment ions is the reason for this. The minimum at the center of the peak is a consequence of the fact that fragment ions which repel each other perpendicularly to the direction of the electrostatic sector field cannot pass the exit slit and thus will not be detected. Moreover, it is possible to de-

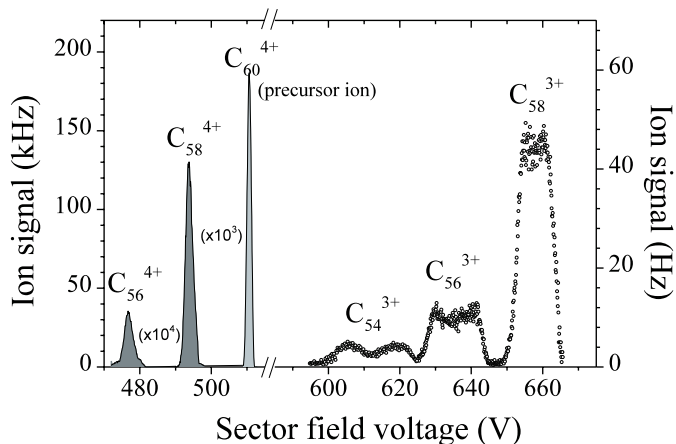


**Fig. 1.** MIKE spectrum of the  $C_{60}^{4+}$  parent ion and its fragment ions. Notice the large peak width of the triply charged fragment ions; this is a result of the Coulomb repulsion. It is possible to determine from the width the kinetic energy which is released in the fragmentation process.

termine the distance between the two fragment ions at the instant of their formation if the interaction potential between the two ions is known [10]. We used three different possible potential curves [11]. In the first approach, the ions are assumed to be point charges. In the second curve, the charges on the larger fragment are moveable on the surface of the fullerene, and localize themselves at positions where the Coulomb energy becomes a minimum. Finally, the third potential curve treats the fullerene as a charged metallic sphere. In this case, the ejected small fragment ion creates an image charge in the fullerene at close distances; this leads to an attractive force.

Figure 2 shows the potential curves calculated for the two fragment ions,  $C_{54}^{3+}$ , and another small singly charged particle. From the width of the  $C_{54}^{3+}$  peak in the MIKE spectrum, it is possible to deduce the kinetic energy release (KER). Under the assumption that an intact  $C_6^+$  is the second fragment ion, the KER is much smaller than assuming the sequential evaporation of two neutral  $C_2$  units and one  $C_2^+$  ion. As the KER of a neutral  $C_2$  evaporation is independent of the charge state of the precursor ion, and is only about 0.4 eV [12, 13], the width of the MIKE peaks measured in case of charge separation reactions will be determined almost completely by the Coulomb repulsion of the two fragment ions. In Fig. 2, the horizontal lines indicate the KER values determined for the two different decay mechanisms – a sequential  $C_2$  evaporation, and the release of an intact  $C_6^+$ . The intersection of this horizontal line with the potential curves gives the position where the two fragment ions were formed. The assumption of a sequential  $C_2$  evaporation leads to the strange result that the potential curves representing charged conductive sphere and moveable charge are not crossed at all by the high KER value determined from the peak width. Moreover, the potential curve corresponding to ideal point charges shows an intersection at a distance which is inside of the fullerene cage. However, the second fragment ion is treated as a  $C_6^+$  ion, all potential curves cross the corresponding KER

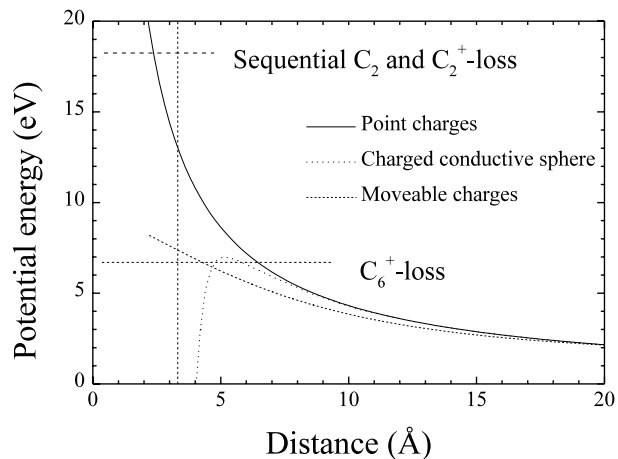


**Fig. 2.** Interaction potentials between a small singly charged ion and a multiply charged fullerene ion  $C_{54}^{3+}$ . The three curves indicate three different approximations for the fullerene ion. The vertical line at a distance of 3.2 Å represents the average cage radius of  $C_{54}$ . The two horizontal lines are the values of the total kinetic energy release (KER) which can be determined from the width of the MIKE peaks shown in Fig. 1. If the singly charged small fragment ion is treated as a  $C_6^+$ , the KER value is almost 3 times lower than that of a sequentially emitted  $C_2^+$ .

line at reasonable distances between the two fragment ions. This is indirect proof that in case of charge separation reactions, the small fragment ion may contain more than two carbon atoms.

The same method used for the measurement of the large fragment ions (see above for the  $C_{54}^{4+}$ ) can be applied in principle for the detection of the smaller fragment ion also. But unfortunately the small fragment ion receives much more of the total KER as a result of the momentum conservation. In case of the dissociation of  $C_{60}^{4+}$  into  $C_{58}^{3+}$  and  $C_2^+$ , the lighter fragment ion gets 29 times more kinetic energy than the heavy  $C_{58}^{3+}$  ion. This leads to several problems that make the observation of the  $C_2^+$  ion very difficult. First, the width of the MIKE peak will be extremely large, and thus the height of the peak will be small; second, the acceptance angle for the  $C_2^+$  ion will be very small, so the minimum at the center of the peak will be much more pronounced as compared to the large fragment ions. In addition, the detection efficiency for a  $C_2^+$  ion, which hits a conversion dynode, is much smaller than that of the  $C_{58}^{3+}$  ion, which is formed in the same dissociation reaction (both fragment ions have about the same velocity as the precursor ion). Measurements of the electron emission statistics of carbon cluster ions hitting a clean gold surface show that the average number of electrons per ion at a given velocity is directly proportional to the number of carbon cluster constituents [14]. Because of these facts, it is not possible to observe the  $C_2^+$  fragment ion in a MIKE spectrum. In the case of a possible decay of  $C_{60}^{4+}$  into  $C_{54}^{3+}$  and  $C_6^+$ , the situation is more favorable, because the mass ratio of the fragment ions is only 9. As compared to the production of a  $C_2^+$  fragment ion this will reduce the width of the MIKE peak of the lighter fragment ion  $C_6^+$ , and the acceptance angle will be increased. Furthermore, the average

number of ejected electrons for a  $C_6^+$  fragment ion having the same velocity as its precursor ion  $C_{60}^{4+}$  is approximately three times that of a  $C_2^+$  fragment ion. Therefore, we are indeed able to observe a MIKE peak for the fragment ion  $C_6^+$  [15]. Moreover, the KER determined from the width of this peak is in good agreement with the KER determined from the width of the  $C_{54}^{3+}$  fragment ion. In addition, the areas of the two fragment ion peaks  $C_{54}^{3+}$  and  $C_6^+$  are more or less the same, if one takes into consideration the smaller acceptance angle and the smaller detection efficiency for the lighter particle.

### 3 Sequential decay reactions

In contrast to these observations, we could also observe sequential  $C_2$  loss of both neutral [16] and charged [17] particles. In the case that the charge of the precursor ion stays completely on the larger fragment ion, it could be shown that sequential  $C_2$  evaporation is the dominant process for the production of fragment ions  $C_m^{z+}$  from a precursor ion  $C_n^{z+}$ , with  $m < n - 2$ .

### 4 Electron emission by surface impact

Besides these studies, which were performed on free molecules in the gas phase, we investigated processes which are induced by the impact of fullerene ions on a metallic surface. The first property we looked at was the secondary electron emission statistics induced by the impact of carbon cluster ions on a clean polycrystalline gold surface. The secondary electron emission can be described by two different mechanisms [18]. One is the result of the transfer of kinetic energy of a projectile electron to electrons in the conduction band of the surface, or kinetic emission. This part of the secondary electron emission is strongly dependent on the velocity of the projectile. This effect is used by many particle detectors in case of large molecules or clusters. A strong post-acceleration of the ion will lead to higher probability of secondary electrons and thus higher detection efficiency. The other mechanism leads to Auger electrons, which can be observed if the potential energy of the projectile is larger than twice the work function of the surface.

Figure 3 shows as an example the average number of electrons per incident ion as a function of the projectile velocity for sodium and neon [19]. Whereas the electron yield for sodium continuously decreases with decreasing velocity, the curve for neon stays at about 0.1, even at very small velocities. This is due to the fact that the ionization energy of neon is larger than twice the work function of the surface used, which is, in the present case, gold. The ionization energies of fullerenes were investigated in detail both theoretically and experimentally [20]. In case of quintuply charged fullerenes, the total ionization energy is on the order of 50 eV and thus much larger than the potential energy of Ne. Therefore, one would expect that such highly charged fullerenes show clear evidence of potential

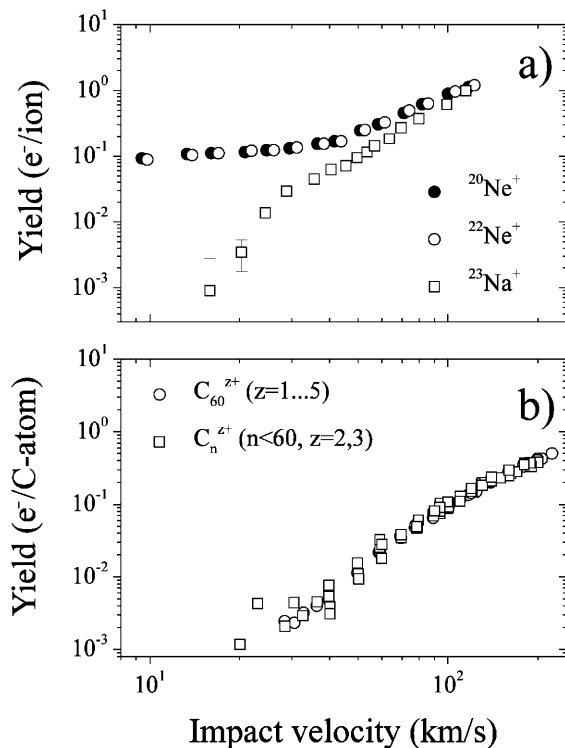


**Fig. 3.** The average number of emitted electrons (=yield) is plotted versus the projectile velocity. The upper part (a) shows the yield per ion of the atomic projectiles  $Ne^+$  and  $Na^+$ , respectively. One can clearly see that singly charged neon atoms emit electrons even if they hit the surface (in the present case, a clean polycrystalline gold surface) at very low velocities. The emission of secondary electrons which is independent of the velocity of the ions, is called potential emission. These data have been taken from Lakits *et al.* [19] and Winter *et al.* [14]. The lower part (b) shows the yield per carbon atom of differently sized and charged fullerene ions. The yield for these fullerene ions shows no potential emission.

emission. Surprisingly, all fullerene ions show exactly the same electron emission yield as a function of the velocity when the yield is normalized to the cluster size (see Fig. 3). A possible explanation for this is the fast transfer of electronic energy (due to the neutralization) into vibrational degrees of freedom. Molecular dynamics calculations appear to support this idea [21].

### 5 Surface-induced reactions

A recently constructed new experimental setup allows us to measure secondary ions, which are formed by the impact of a mass-selected ion on a metallic surface, as a function of the impact energy [22]. The energy resolution of this experimental setup is on the order of 100 meV, in case of molecular projectiles. The secondary ion mass spectra obtained from singly charged fullerenes are in good agreement with the literature [23]. Up to about 250 eV, fullerene ions show no fragmentation, and only the reflected primary

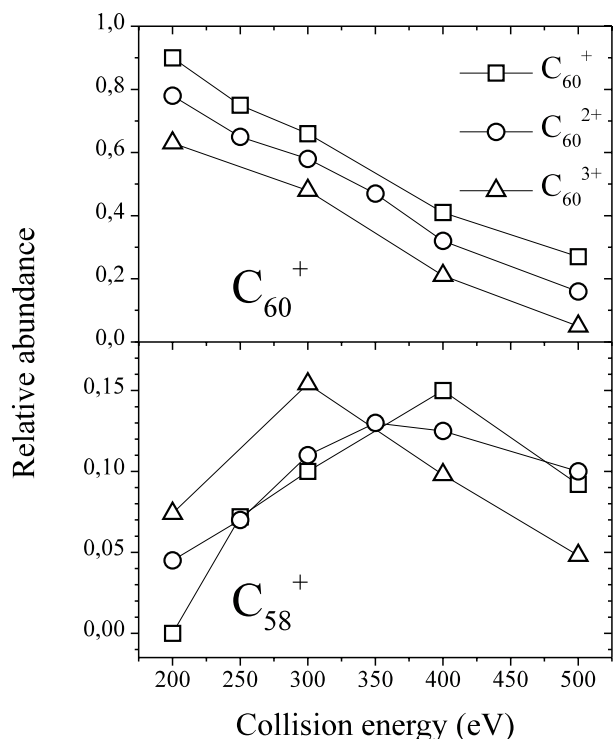


**Fig. 4.** Secondary ions were investigated upon the collision of differently charged  $C_{60}$  ions with a stainless steel surface. The relative ion intensity versus the impact energy is plotted. The upper part shows the nonfragmented singly charged  $C_{60}$  secondary ion. There is a well-pronounced shift of the ion intensity of about 50 eV to the left when the charge state of the primary ion is increased by 1. The same shift of 50 eV can be seen in the lower part for the maxima of the  $C_{58}^+$  secondary ion signal.

ion can be observed. In contrast to the studies already published, we were also interested in the secondary ion mass spectra of highly charged fullerenes. Figure 4 shows the relative intensity of two different singly charged secondary ions (no multiply charged secondary ions have been observed) as a function of the impact energy for singly, doubly, and triply charged fullerene primary ions. The different symbols are for the different charge states of the primary ion  $C_{60}^{z+}$  (with  $z = 1$  to 3). The intact  $C_{60}^+$  secondary ion yield decreases continuously with increasing impact energy for all charge states (see upper part of Fig. 4). It can be seen that the relative ion intensity of the  $C_{60}^+$  secondary ion is smaller at the same impact energy for more highly charged precursor ions. This explains qualitatively that the neutralization by a surface collision indeed leads to a stronger fragmentation. The horizontal shift of the curves is about 50 eV. The same shift of 50 eV can be seen in the maximum of the  $C_{58}^+$  ion signal shown in the lower part of the figure. As only about 10%–20% of the collision energy will be transferred into internal energy [24] the difference in the internal energy between the different charge states will be on the order of 10 eV. This is in very good agreement with the ionization energies determined for  $C_{60}$  in different charge states.

This work was supported by the FWF, OENB, and BMWV, Wien, Austria. One of us (P.S.) thanks the Austrian Academy of Sciences for being a fellow of APART.

## References

1. H.W. Kroto, J.R. Heath, S.C. O'Brien, R.F. Curl, R.E. Smalley: *Nature* **318**, 162 (1985)
2. R.D. Beck, P.S. John, M.M. Alvarez, F. Diederich, R.L. Whetten: *J. Phys. Chem.* **95**, 8402 (1991)
3. C.I. Frum, R. Engelman, H.G. Hedderich, P.F. Bernatz, L.D. Lamb, D.R. Hoffman: *Chem. Phys. Lett.* **176**, 504 (1991)
4. M. Foltin, M. Lezius, P. Scheier, T.D. Märk: *J. Chem. Phys.* **98**, 9624 (1993)
5. J. Jin, H. Khemliche, M.H. Prior, Z. Xie: *Phys. Rev. A* **53**, 615 (1996)
6. P. Scheier, T.D. Märk: *Phys. Rev. Lett.* **73**, 54 (1994)
7. M. Foltin, O. Echt, P. Scheier, B. Dünser, R. Wörgötter, D. Muigg, S. Matt, T.D. Märk: *J. Chem. Phys.* **107**, 6246 (1997)
8. J. Opitz, B.A. Huber: "Similarities and differences in atomic nuclei and clusters", in *Proceedings of the API Conference* **416**, 422 (1998)
9. P. Scheier, B. Dünser, R. Wörgötter, S. Matt, D. Muigg, G. Senn, T.D. Märk: *Int. Rev. Phys. Chem.* **15**, 93 (1996)
10. P. Scheier, B. Dünser, T.D. Märk: *Phys. Rev. Lett.* **74**, 3368 (1995)
11. G. Senn, T.D. Märk, P. Scheier: *J. Chem. Phys.* **108**, 990 (1998)
12. S. Matt, M. Sonderegger, R. David, O. Echt, P. Scheier, J. Laskin, C. Lifshitz, T.D. Märk: *Int. J. Mass Spectrom. Ion Processes* **185/186/187**, 813 (1999)
13. C. Lifshitz, M. Iraqi, T. Peres, J.E. Fischer: *Int. J. Mass Spectrom. Ion Processes* **107**, 565 (1991)
14. HP. Winter, M. Vana, G. Betz, F. Aumayr, H. Drexel, P. Scheier, T.D. Märk: *Phys. Rev. A* **56**, 3007 (1997)
15. P. Scheier, G. Senn, S. Matt, T.D. Märk: *Int. J. Mass Spectrom. Ion Processes* **172** (1998) L1
16. P. Scheier, B. Dünser, R. Wörgötter, D. Muigg, S. Matt, O. Echt, M. Foltin, T.D. Märk: *Phys. Rev. Lett.* **77**, 2654 (1996)
17. B. Dünser, O. Echt, P. Scheier, T.D. Märk: *Phys. Rev. Lett.* **79**, 3861 (1997)
18. G. Höhler (ed.): *Particle-induced Electron Emission*, Vol. I and II (Springer, Heidelberg 1992)
19. G. Lakits, F. Aumayr, M. Heim, HP. Winter: *Phys. Rev. A* **42**, 5780 (1990)
20. S. Matt, O. Echt, R. Wörgötter, V. Grill, P. Scheier, C. Lifshitz, T.D. Märk: *Chem. Phys. Lett.* **264**, 149 (1997) and references therein
21. F. Aumayr, G. Betz, T.D. Märk, P. Scheier, HP. Winter: *Int. J. Mass Spectrom. Ion Processes* **174**, 317 (1998)
22. R. Wörgötter, C. Mair, T. Fiegele, V. Grill, T.D. Märk, H. Schwarz: *Int. J. Mass Spectrom. Ion Processes* **164**, L1 (1997)
23. R.D. Beck, J. Rockenberger, P. Weis, M.M. Kappes: *J. Chem. Phys.* **104**, 3638 (1996)
24. R.G. Cooks, T. Ast, M.A. Mabud: *Int. J. Mass Spectrom. Ion Processes* **100**, 209 (1990)